PROCEEDINGS OF SCIENCE

Search for a gamma-ray line feature with DAMPE

Zhao-Qiang Shen[*a], **Yun-Feng Liang**[a], **Kai-Kai Duan**[ab], **Xiang Li**[a] **and Yi-Zhong Fan**[ac] **on behalf of the DAMPE Collaboration**[†]

[a] *Key Laboratory of Dark Matter and Space Astronomy, Purple Mountain Observatory, Chinese Academy of Sciences, Nanjing 210033, China*

[b] *University of Chinese Academy of Sciences, Beijing, 100012, China*

[c] *School of Astronomy and Space Science, University of Science and Technology of China, Hefei, 230026, China*

E-mail: zqshen@pmo.ac.cn, liangyf@pmo.ac.cn, xiangli@pmo.ac.cn

DArk Matter Particle Explorer (DAMPE) measures the gamma rays with an excellent energy resolution. Therefore, DAMPE is suitable for the search of gamma-ray line emission that could arise from dark matter annihilation or decay. We have analyzed the Galactic center and nearby galaxy clusters with 3 years of DAMPE data. No statistically significant line is identified between 10 GeV and 300 GeV and we present the 95% confidence limits of the velocity-averaged cross section for dark matter particle annihilation into a pair of gamma rays.

36th International Cosmic Ray Conference -ICRC2019-
July 24th - August 1st, 2019
Madison, WI, U.S.A.

[*] Speaker.

[†] for collaboration list see PoS(ICRC2019)1177

PoS(ICRC2019)601

1. Introduction

Dark matter (DM) is an important component in the Universe, which accounts for 26.5% of the mean energy density today [1] and provides additional gravitational force in various places of different scales [2]. Weakly interacting massive particles (WIMPs) are favorable DM candidates, whose mass is in the range of 10 GeV $-$ 1 TeV [3]. If a pair of WIMPs (χ) can annihilate into a photon (γ) and another particle (X) directly, a line structure at $E_\gamma = m_\chi\,(1 - m_X^2/4m_\chi^2)$ may be observed. Furthermore, the internal bremsstrahlung process during the annihilation of DM particles can also create a sharp feature in the gamma-ray band [4]. Since the line-like spectrum is hard to be produced in known astrophysical processes, a robust detection of it would be a smoking-gun signature of WIMPs.

Great efforts have been paid in searching for lines in the Fermi era, but no line signal is significantly detected (see [5] for a recent review). Nevertheless two line candidates are reported in the literature. The $\sim$ 130 GeV line was firstly suggested in the Galactic center (GC) [4, 6] and also shown in the galaxy clusters (GCls) [7]. However, it was not confirmed by the Fermi-LAT pass 8 data [8]. In addition, by analyzing the 16 GCls selected from the HIFLUGCS catalog with large J-factors [9], a tentative line at $\sim$ 43 GeV was identified [10]. Since these candidates are weak and may potentially be caused by instrumental uncertainties, line searches in the same energy range using another telescope are quite necessary.

The DArk Matter Particle Explorer (DAMPE) is a space-borne high energy particle detector dedicated to measure cosmic rays and photons in a broad energy range [11, 12, 13]. It is made by a Plastic Scintillator strip Detector (PSD), a Silicon-Tungsten tracker-converter (STK), a BGO imaging calorimeter and a Neutron Detector (NUD). This telescope has a great potential in searching for the monochromatic and/or sharp spectral structures in GeV$-$TeV range thanks to its excellent energy resolution. DAMPE may also be helpful in studying the high-energy gamma-ray sources, such as Active Galactic Nuclei (AGN), the Crab flares and some bright gamma-ray bursts [12, 14, 15].

In this work, we will use 3 years of DAMPE data to search for line structures from 10 to 300 GeV in GC and some nearby GCls. The constraints on the velocity-averaged WIMPs annihilation cross section will also be presented using the upper limits derived in the GC.

2. DAMPE data selection

We use the gamma-ray photons selected from the DAMPE flight data observed from 2016-01-01 to 2019-01-01 [16]. In order to balance the energy resolution and exposure, we only include in our analysis the photons which both satisfy the High Energy trigger (HET) condition and have incident angles less than 38°. We also drop those events when the satellite is in the South Atlantic Anomaly (SAA) region or a strong solar flare happening between 2017-09-08 and 2017-09-14. Since the sliding window analysis (see the following sections for detail) is performed in this work, we choose a wider energy range, from 5 to 450 GeV, to better fit the background spectrum in the lowest or highest energy bins. Throughout our analysis, the scientific tools and the Monte Carlo (MC) derived instrumental response functions (IRFs) provided by `DmpST` are adopted [17].

Fig. 1 shows the spectral energy distribution (SED) of the resultant data set after masking $|b| < 5°$ and $|l| > 6°$ which reduces the astrophysical background. In order to derive the exposure,

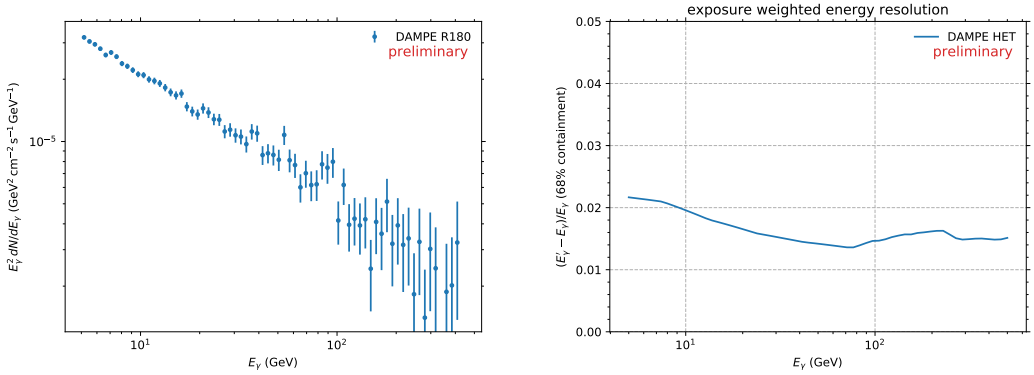

Figure 1: The spectral energy distribution (SED) of the DAMPE photons after masking the Galactic plane (left panel) and the exposure weighted energy resolution (68% containment) at the Galactic center (right panel).

we first calculate the integrated livetime for the entire sky as a function of the inclination angle using the pointing information of DAMPE, and then add up the product of livetime and effective area of different inclination angles. We find that the SED is generally a power-law spectrum and no significant line-like structure exists.

We also calculate the exposure weighted energy resolution (half of the 68% energy dispersion fractional containment) between 5 and 500 GeV based on the livetime at the GC and MC IRFs [17] as given in the right panel of Fig. 1. The energy resolution of our data set is approximately $2\% - 2.2\%$ below 10 GeV and gradually decreases to $\sim 1.5\%$. Please note that the photon selection algorithm of our data set is not optimized for the line search [16], therefore a data set with smaller energy dispersion is still possible.

3. Line search in the Galactic center

Since the GC is expected to have a great amount of DM and is rather close to the solar system, it is often considered as one of the most promising places to find DM annihilation signals. However complex astrophysical backgrounds also exist there. In order to improve the sensitivity, we choose the region of interest (ROI) set defined in [6] as listed in Tab. 1 considering the uncertainties of DM distribution. To recap briefly, the ROIs with different radii centering at the GC are created according to the DM density profiles and the Galactic plane region distant from the GC ($|b| < 5^\circ$ and $|l| > 6^\circ$) is excluded. For a concentrated density profile such as contracted Navarra-Frenk-White (contracted NFW; NFWc) profile, DM signal is less likely affected by the background, so a smaller ROI is used; while for the flat distribution such as isothermal profile, larger ROI is needed to include more signal events (see [6] and the references therein for DM profiles).

We adopt the sliding windows technique to search for the line-like signal quantitatively [4]. The main idea of it is to analyze a series of lines in a smaller energy window around the line, which will help to decrease the bias from the inaccurate background spectral model, since in a narrow range the background spectrum can well be approximated by a simple power law model. We choose a set of line energies $E_{\rm line}$ between 10 and 300 GeV with the difference between two

Profile	ROI	J-factor (10^{22} GeV^2 cm^{-5} sr)
NFWc	R3	13.9
Einasto	R16	8.48
NFW	R41	8.53
Isothermal	R90	6.94

Table 1: The optimized ROIs and J-factors for the four DM density profiles considering the DM annihilation [6]. In the table Rx means a $R = x^\circ$ ROI centering at the GC excluding the Galactic plane.

adjacent lines being $0.5\sigma_E$, where σ_E is the half width of the 68% exposure weighted energy dispersion containment at the GC. The energy window is from $0.5E_{\rm line}$ to $1.5E_{\rm line}$ [8, 10].

In each window, the unbinned likelihood method is adopted [18], which can avoid the uncertainties caused by the binning scheme. The likelihood function $L(\Theta)$ in the energy range of $[E_{\rm min}, E_{\rm max}]$ is defined as

$$\ln L(\Theta) = \sum_{i=1}^{N_{\rm ph}} \ln[\bar{\lambda}(E_i;\Theta)] - \int_{E_{\rm min}}^{E_{\rm max}} \bar{\lambda}(E;\Theta)\,{\rm d}E, \tag{3.1}$$

where $N_{\rm ph}$ is the number of observed photons in the energy window, $\bar{\lambda}(E;\Theta)$ is the expected counts in model per energy range with the parameter Θ, which is calculated with the exposure $\bar{\varepsilon}(E)$ at energy E averaged over the ROI.

We perform a likelihood ratio test [19] in each window to check whether or not the line structure at $E_{\rm line}$ exists. The null hypothesis consists of a power-law background, i.e. $\bar{\lambda}_{\rm null}(E) = F_{\rm b}(E)\,\bar{\varepsilon}(E)$, and the signal hypothesis consists of a monochromatic line and a background component, i.e. $\bar{\lambda}_{\rm sig}(E) = F_{\rm b}(E)\,\bar{\varepsilon}(E) + F_{\rm s}(E)\,\bar{\varepsilon}(E_{\rm line})$ [10]. The power-law spectrum and the line structure are written as $F_{\rm b}(E;N_{\rm b},\Gamma) = N_{\rm b}\,E^{-\Gamma}$ and $F_{\rm s}(E;N_{\rm s},E_{\rm line}) = N_{\rm s}\,D_{\rm eff}(E;E_{\rm line})$ (i.e. $S_{\rm line}(E) = N_{\rm s}\,\delta(E-E_{\rm line})$ without energy dispersion) respectively, where $D_{\rm eff}$ is the exposure weighted energy dispersion function averaged over the ROI (see [17] for detail). We fit both the hypotheses to the data with `MINUIT` [20] and calculate the test statistic (TS) value ${\rm TS} \equiv -2\,(\ln L_{\rm null} - \ln L_{\rm sig})$ in each window. The TS values of a series of line energies is drawn in the left panels of Fig. 2. We do not find any significant line structure in our analysis, with the largest TS value being 8.88 at 37.7 GeV in the R16 ROI which is less than 3σ local significance.[1]

Since no line signal is found by DAMPE, we calculate the 95% confidence level upper limits on the DM annihilation cross section by using the formula

$$S_{\rm line}(E) = \frac{1}{4\pi}\frac{\langle\sigma v\rangle_{\chi\chi\to\gamma\gamma}}{2m_\chi^2}\,2\delta(E-E_{\rm line})\,J, \tag{3.2}$$

where m_χ is the rest mass of DM particle, $\langle\sigma v\rangle_{\chi\chi\to\gamma\gamma}$ is the velocity-averaged annihilation cross section, $E_{\rm line}$ is the energy of monoenergetic photons, and J is the J-factor of Galactic DM halo within the ROI. Finally the obtained results are shown in the right panels of Fig. 2. Compared with the constraints from the 5.8-year Fermi-LAT data in [8], we find our upper limits several times weaker in the small ROIs such as R3 and R16, since Fermi-LAT has more exposure at GC.

[1] No look-elsewhere effect is considered in calculating the local significance.

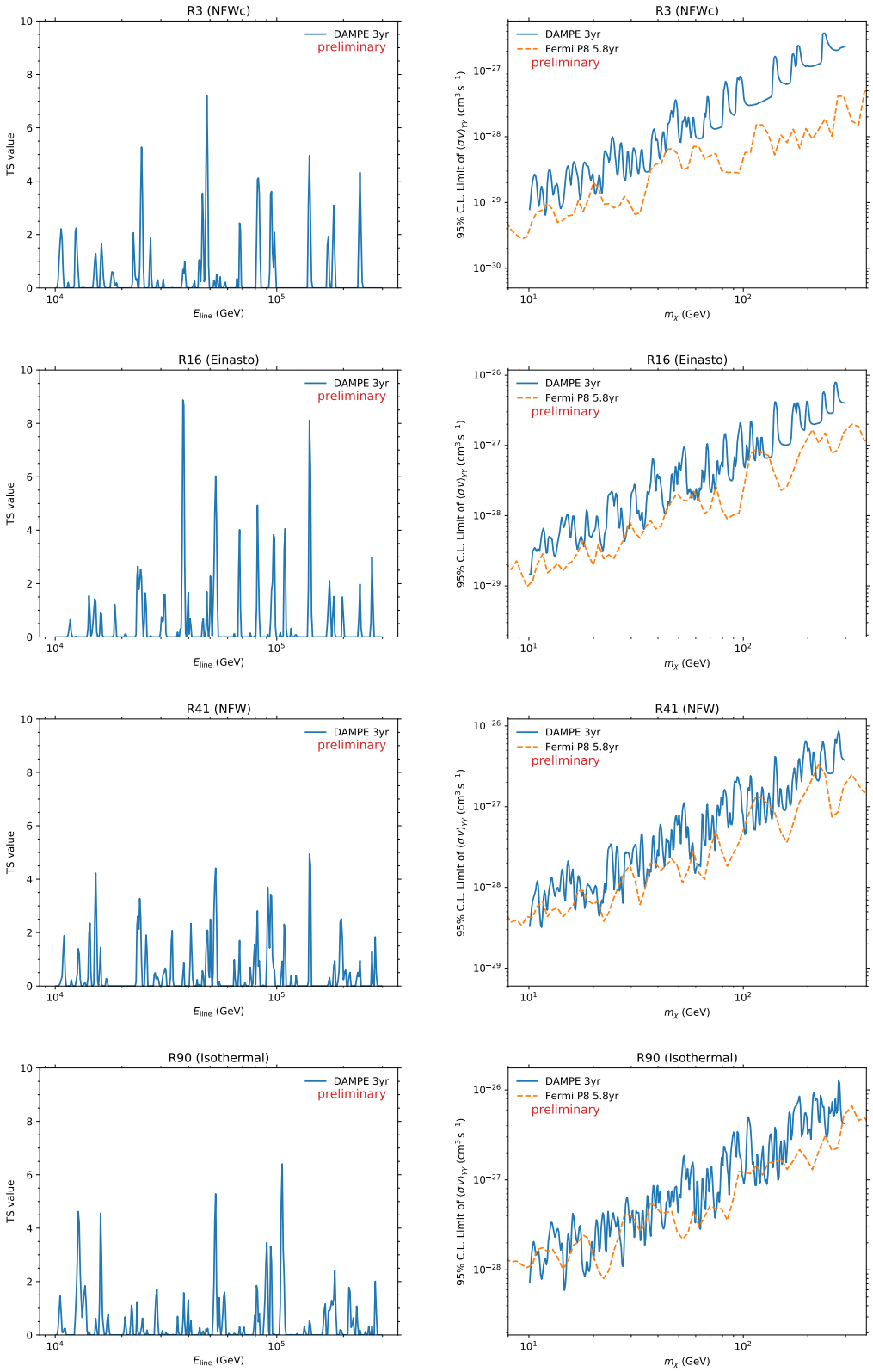

Figure 2: The TS values of a series of line energies in the sliding window analysis of the GC (left panels) and the 95% confidence level upper limits on the DM annihilation cross section (right panels). The figures from top to bottom correspond to the ROIs denoted as R3, R16, R41 and R90 respectively.

However, our constraint is quite close to that of Fermi-LAT for R90 ROI thanks to the excellent energy resolution.

4. Line search in nearby galaxy clusters

GCls are the largest gravitational bound system in the Universe and most of their mass is contributed by dark matter [9]. Also since lots of subhalos are expected in the smooth dark matter halo of the clusters (e.g. [21]), the dark matter signal can be boosted by a factor of $\sim 30-1000$ [22, 23]. Therefore, GCls are also good targets for the dark matter indirect search.

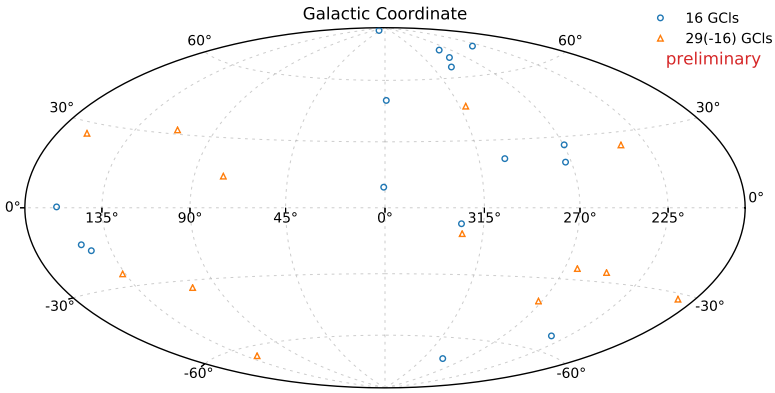

Figure 3: The galaxy cluster (GCl) samples we used in the analysis. The blue circles show the 16 GCls the same as that of [9]. All the markers (both circles and triangles) represent the 29 GCls with large J-factors in the HIFLUGCS.

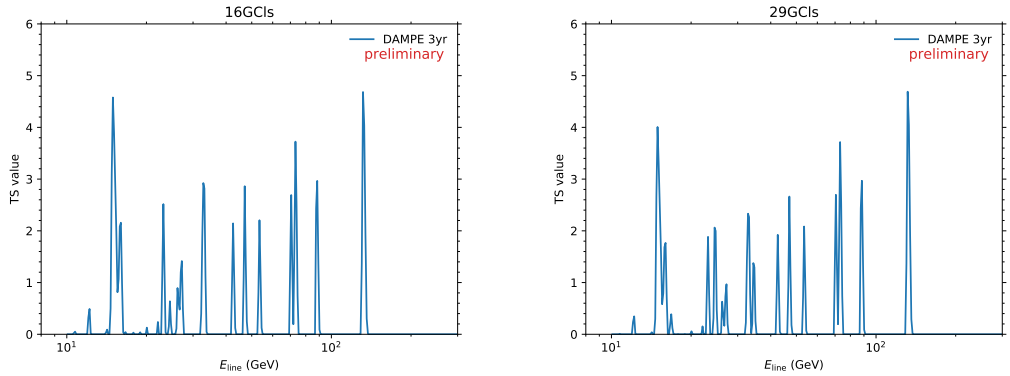

Figure 4: The TS values of a series of line energies in the sliding window analysis of the 16 GCls (left panel) and 29 GCls (right panel).

In this work, we use two GCl samples selected from the HIFLUGCS catalog [24, 25] as shown in Fig. 3. One first sample is the same as that of [9], which contains 16 GCls with large J-factors including 3C 129, A1060, A1367, A2877, A3526, A3627, AWM 7, Coma, Fornax, M49, NGC 4636, NGC 5813, Ophiuchus, Perseus, S 636 and Virgo. We also create another GCl sample by adding A0119, A0262, A0576, A0754, A2256, A2319, A2634, A3266, A3376, A3395s,

NGC 1550, NGC 5044 and Triangulum to the above sample to increase statistics.[2] We use 2.6° and 1.7° as the radii of Virgo and M49 respectively to avoid overlapping [10] and define the ROIs of other sources according to their R_{200} radii.

By stacking the photons in each GCl sample and performing the unbinned sliding window analysis similar to that introduced in Sec. 3, we derived the TS values of line structures as shown in Fig. 4. Still no lines are significantly found in the energy range of $10-300$ GeV.

5. Conclusions

Thanks to the excellent energy resolution, DAMPE has an advantage in line searches. In this work, we perform unbinned analyses in both the GC and nearby GCls, which potentially have DM annihilation signals, using 3 years of DAMPE photons. No statistically significant line structures are found between 10 GeV and 300 GeV in these sources, therefore the 95% upper limits of DM annihilation cross section to a pair of photons based on the analysis of GC are derived. We find the upper limits using a large ROI have a similar constraint as that derived from 5.8 years of Fermi-LAT data in [8]. However since Fermi-LAT has more exposure in the GC, our constraints for the small ROIs (e.g. R3 and R16) are still weaker than that of Fermi-LAT. More gamma-ray photons and a data set optimized for the energy resolution are needed for further improvements.

Acknowledgments

The DAMPE mission is funded by the strategic priority science and technology projects in space science of Chinese Academy of Sciences. In China the data analysis is supported in part by the National Key Research and Development Program of China (No. 2016YFA0400200), the National Natural Science Foundation of China (Nos. 11525313, 11622327, 11722328, U1738205, U1738207, U1738208, 11851305), the strategic priority science and technology projects of Chinese Academy of Sciences (No. XDA15051100), the 13th Five-Year Informatization Plan of Chinese Academy of Sciences (No. XXH13506), the 100 Talents Program of Chinese Academy of Sciences, and the Young Elite Scientists Sponsorship Program. In Europe the activities and the data analysis are supported by the Swiss National Science Foundation (SNSF), Switzerland; the National Institute for Nuclear Physics (INFN), Italy.

References

[1] N. Aghanim *et al.* (Planck Collaboration), *Planck 2018 results. VI. Cosmological parameters*, *Astron. Astrophys.* (2018) [arXiv:1807.06209].

[2] G. Bertone and D. Hooper, *History of dark matter*, *Rev. Mod. Phys.* **90**, 045002 (2018).

[3] J. L. Feng, *Dark Matter Candidates from Particle Physics and Methods of Detection*, *Annu. Rev. Astron. Astrophys.* **48**, 495 (2010).

[4] T. Bringmann, X. Huang, A. Ibarra, S. Vogl, and C. Weniger, *Fermi LAT search for internal bremsstrahlung signatures from dark matter annihilation*, *J. Cosmol. Astropart. Phys.* **07** (2012) 054.

[5] E. Charles, M. Sánchez-Conde, B. Anderson *et al.*, *Sensitivity projections for dark matter searches with the Fermi large area telescope*, *Phys. Rep.* **636**, 1 (2016).

[2] We do not include A2199 and A3571 since no photons are detected by DAMPE within their ROIs.

[6] M. Ackermann *et al.* (Fermi-LAT Collaboration), *Search for gamma-ray spectral lines with the Fermi Large Area Telescope and dark matter implications*, *Phys. Rev. D* **88**, 082002 (2013).

[7] A. Hektor, M. Raidal, and E. Tempel, *Evidence for Indirect Detection of Dark Matter from Galaxy Clusters in Fermi γ-ray Data*, *Astrophys. J. Lett.* **762**, L22 (2013).

[8] M. Ackermann *et al.* (Fermi-LAT Collaboration), *Updated search for spectral lines from Galactic dark matter interactions with pass 8 data from the Fermi Large Area Telescope*, *Phys. Rev. D* **91**, 122002 (2015).

[9] B. Anderson, S. Zimmer, J. Conrad *et al.*, *Search for gamma-ray lines towards galaxy clusters with the Fermi-LAT*, *J. Cosmol. Astropart. Phys.* **02** (2016) 026.

[10] Y.-F. Liang, Z.-Q. Shen, X. Li, Y.-Z. Fan *et al.*, *Search for a gamma-ray line feature from a group of nearby galaxy clusters with Fermi LAT Pass 8 data*, *Phys. Rev. D* **93**, 103525 (2016).

[11] J. Chang, *Dark Matter Particle Explorer: The First Chinese Cosmic Ray and Hard γ-ray Detector in Space*, *Chin. J. Spac. Sci.* **34**, 550 (2014).

[12] J. Chang *et al.* (DAMPE Collaboration), *The DArk Matter Particle Explorer mission*, *Astropart. Phys.* **95**, 6 (2017).

[13] G. Ambrosi *et al.* (DAMPE Collaboration), *The on-orbit calibration of DArk Matter Particle Explorer*, *Astropart. Phys.* **106**, 18 (2019).

[14] S.-J. Lei, Q. Yuan, Z.-L. Xu, K.-K. Duan, and M. Su, *Gamma-ray Astronomy with DAMPE*, in proceedings of *ICRC2017*, PoS(ICRC2017)616 (2017).

[15] X. Li, K.-K. Duan, W. Jiang, Z.-Q. Shen, and M. M. Salinas, *Recent γ-ray Results from DAMPE*, in proceedings of *ICRC2019*, PoS(ICRC2019)576 (2019).

[16] Z.-L. Xu, K.-K. Duan, Z.-Q. Shen *et al.*, *An algorithm to resolve γ-rays from charged cosmic rays with DAMPE*, *Res. Astron. Astrophys.* **18**, 027 (2018).

[17] K.-K. Duan, W. Jiang, Y.-F. Liang *et al.*, *DmpIRFs and DmpST: DAMPE Instrument Response Functions and Science Tools for Gamma-Ray Data Analysis*, *Res. Astron. Astrophys.* **19**, 132 (2019).

[18] J. R. Mattox, D. L. Bertsch, J. Chiang *el al.*, *The Likelihood Analysis of EGRET Data*, *Astrophys. J.* **461**, 396 (1996).

[19] W. Cash, *Parameter Estimation in Astronomy through Application of the Likelihood Ratio*, *Astrophys. J.* **228**, 939 (1979).

[20] F. James and M. Roos, *Minuit - a system for function minimization and analysis of the parameter errors and correlations*, *Comput. Phys. Commun.* **10**, 343 (1975).

[21] L. Gao, J. F. Navarro, C. S. Frenk, A. Jenkins, V. Springel, and S. D. M. White, *The Phoenix Project: the dark side of rich Galaxy clusters*, *Mon. Not. R. Astron. Soc.* **425**, 2169 (2012).

[22] L. Gao, C. S. Frenk, A. Jenkins, V. Springel, and S. D. M. White, *Where will supersymmetric dark matter first be seen?*, *Mon. Not. R. Astron. Soc.* **419**, 1721 (2012).

[23] M. A. Sánchez-Conde and F. Prada, *The flattening of the concentration–mass relation towards low halo masses and its implications for the annihilation signal boost*, *Mon. Not. R. Astron. Soc.* **442**, 2271 (2014).

[24] T. H. Reiprich and H. Böhringer, *The Mass Function of an X-Ray Flux-limited Sample of Galaxy Clusters*, *Astrophys. J.* **567**, 716 (2002).

[25] Y. Chen, T. H. Reiprich, H. Böhringer, Y. Ikebe, and Y.-Y. Zhang, *Statistics of X-ray observables for the cooling-core and non-cooling core galaxy clusters*, *Astron. Astrophys.* **466**, 805 (2007).